ELSEVIER

Journal of Organometallic Chemistry 518 (1996) 85–95

Journal of Organometallic Chemistry

X-ray crystallographic studies and comparative reactivity studies of a sodium diisopropylamide (NDA) complex and related hindered amides

Philip C. Andrews [a,*,1], Nicholas D.R. Barnett [a], Robert E. Mulvey [a], William Clegg [b], Paul A. O'Neil [b], Donald Barr [c], Lucy Cowton [c], Andrea J. Dawson [d], Basil J. Wakefield [d]

[a] *Department of Pure and Applied Chemistry, University of Strathclyde, Glasgow G1 1XL, UK*
[b] *Department of Chemistry, University of Newcastle, Newcastle upon Tyne NE1 7RU, UK*
[c] *The Associated Octel Company Ltd., Ellesmere Port, South Wirral L65 4HF, UK*
[d] *Department of Chemistry and Applied Chemistry, University of Salford, Salford M5 4WT, UK*

Received 15 November 1995

Abstract

Two related sodium amide complexes derived from secondary amines with bulky organic substituents have been synthesised and crystallographically characterised. Both $[(^{i}Pr)_2NNa(TMEDA)]_2$ and $[Cy(^{i}Pr)NNa(TMEDA)]_2$ adopt dimeric crystal structures with a central, planar (nitrogen–metal)$_2$ azametallocycle, a now familiar feature in both lithium amide and sodium amide chemistry. TMEDA ligands chelate in their usual bidentate manner making the Na^+ cations four-coordinate with a distorted tetrahedral geometry. In the latter complex, the amido substituents are disposed in a *trans* conformation with respect to the $(NNa)_2$ ring plane. The deprotonating ability of the former complex has been tested against that of the parent amide $[(^{i}Pr)_2NNa]_\infty$ and the lithium congener $[(^{i}Pr)_2NLi]_\infty$ (LDA) in a series of simple organic reactions: selective enolate formation from 2-octanone and 2-methylcyclohexanone; synthesis of diphenylacetic acid via diphenylmethane. In general, the performance of the sodium reagents compares favourably with that of the lithium reagent.

Keywords: Lithium; Sodium; Amide; Crystal structure

1. Introduction

During the past 15 years there has been quite a significant growth in the structural characterisation of crystalline lithium amides. This reflects their extensive use as synthetic reagents and also the importance of understanding their structures as a guide to explaining their reactivity and selectivity [1].

Hindered lithium amides $[RR'NLi(L)_k]_n$ can have certain advantages over the more conventional alkyllithium reagents such as BuLi or MeLi when utilised in proton abstraction reactions. They can react in a highly regio- and stereospecific manner and their high basicity and low nucleophilicity make them particularly useful in reactions with organic substrates containing carbonyl or other such unsaturated functional groups [2]. The most widely utilised reagent in this respect is lithium diisopropylamide (LDA). Although not yet comprehensive, a good deal of information now exists on both its solution [3] and solid state structures [4]. When not complexed by Lewis base donor molecules it exists in the solid state as a helical polymer [5], although it has previously been described in solution as being in the form of various cyclic oligomers. On complexation with TMEDA (N,N,N′,N′-tetramethylethylenediamine) it crystallises as the polymer $\{[(^{i}Pr)_2NLi]_2(TMEDA)\}_\infty$ [6], and with THF as the dimer $[(^{i}Pr)_2NLi(THF)]_2$ [7]. LDA has also been characterised in the solid state within mixed-anion species, e.g. $\{[(^{i}Pr)_2NLi]_2LiCl(TMEDA)_2\}$ [8].

In this paper, we report the first crystal structure of a sodium diisopropylamide (NDA) complex, $[(^{i}Pr)_2NNa(TMEDA)]_2$ **1**, along with the closely related structure of the isopropylcyclohexylamide $[Cy(^{i}Pr)NNa(TMEDA)]_2$ **2**. Such heavier alkali metal amides potentially offer enhanced reactivity over their lithium counterparts in proton abstraction applications, though this may be achieved with a loss in selectivity. In order to explore

* Corresponding author.
[1] Present address: Department of Chemistry, Monash University, Clayton, Victoria 3168, Australia.

PII S0022-328X(96)06203-1

this possibility we have performed studies measuring the relative performance of lithium and sodium diisopropylamides in simple reactions reported by Corey and Gross [9] and Brandsma [10] involving selective enolate formation, and also in the metallation of diphenylamine.

2. Sodium amide complexes 1 and 2

2.1. Results and discussion

The two methods which we utilised in the synthesis of the sodium amides are represented schematically in Eqs. (1), (2) and (3):

$$^{n}BuLi + NaO^{t}Bu \xrightarrow{i,\ ii} {}^{n}BuNa\downarrow + LiO^{t}Bu \quad (1)$$

i = hexane
ii = 0°C → 25°C, 7 h

$$^{n}BuNa + RR'NH \xrightarrow{i,\ ii} [RR'NNa(L)_k]_n \quad (2)$$

i = hydrocarbon solvent, e.g. pentane, hexane, cyclohexane, heptane
ii = Lewis base(s), (L)
Reaction temperature variable

$$RR'NH + Na(disp) \xrightarrow[iii]{i,\ ii} [RR'NNa(L)_k]_n \quad (3)$$

i = toluene or octane
ii = Lewis base(s), (L)
iii = 25°C

The first method involved the reaction of the pre-dried amine with freshly prepared ^{n}BuNa in hexane or cyclohexane followed by the addition of a stoichiometric amount of an appropriate Lewis base (Eq. (2)). The ^{n}BuNa was prepared beforehand from the transmetallation reaction of commercially available ^{n}BuLi with NaO^{t}Bu in hexane (Eq. (1)). The resultant powder, which is highly pyrophoric when dry, was isolated, washed with hexane and stored under argon in a glove box. Unfortunately, ^{n}BuNa metallates toluene easily and is insoluble in hydrocarbon solvents, however, it is reactive enough to deprotonate most secondary or primary amines in a hexane medium, quickly if the amine is in solution and more slowly if it is a solid. As is found for many sodium amide complexes, a non-polar hydrocarbon solvent was sufficient, with gentle heating, to ensure complete dissolution of complexes **1** and **2**. When this is not the case, then further amounts of polar solvents, e.g. THF, have to be added but, owing to the high reactivity of ^{n}BuNa, it is advisable that this is done only after metallation of the amine has occurred. The second procedure uses elemental sodium in the metallation of the amine (Eq. (3)), as reported in an earlier communication [11]. Under normal circumstances this reaction is very slow or ineffective. However, in the presence of one equivalent of an electron carrier such as isoprene the reaction proceeds efficiently, with or without the presence of a Lewis base. We found the optimum Na dispersion : amine : isoprene ratio to be 1 : 1 : 0.5 and also that the electron carriers styrene, biphenyl and naphthalene were less effective in the preparation of **1**. Both procedures have proved to be highly effective in the synthesis and isolation of microcrystalline or crystalline products in high yield.

Crystals of both **1** and **2** were grown from hexane solutions at ambient temperature (approximately 21°C), **1** as pale red needles and **2** as pale pink blocks. The first batch yield of **1** is relatively low at only 31%; this is not the result of it being a minor solution product nor is it representative of a high degree of solubility, since the microcrystalline product can be extracted at ambient temperature in high yield, usually in the region of 80%. The difficulty therefore was in maintaining the complex in solution long enough so that crystals suitable for X-ray analysis could be grown. NDA will also dissolve in other Lewis bases such as PMDETA (N,N,N′,N′,N″-pentamethyldiethylenetriamine), TEEDA (N,N,N′,N′-tetraethylethylenediamine) and DMPU (1,3-dimethyl-3,4,5,6-tetrahydro-2(1H)-pyrimidinone), but attempts at crystallisation have thus far been unsuccessful. A high yield of crystalline **2** can be obtained by cooling the solution slowly in a water bath from a temperature of 55°C.

Both complexes are, as expected, highly sensitive to air and moisture. However, importantly, they are non-pyrophoric and are stable if stored under argon gas for periods of at least six months. Unlike **2**, which has a sharp melting point of 96–97°C, the crystals of **1** melt over the range 88–94°C.

The crystal structures, shown in Figs. 1 and 2, reveal that **1** and **2** adopt a structural conformation which has been commonly observed not only with lithium amides but also, more recently, among sodium amides. Most sodium amides structurally characterised to date contain the core features adopted by **2** of a central planar four-membered (amido N–Na)$_2$ ring with the organic substituents extending out from the ring in a *transoid*

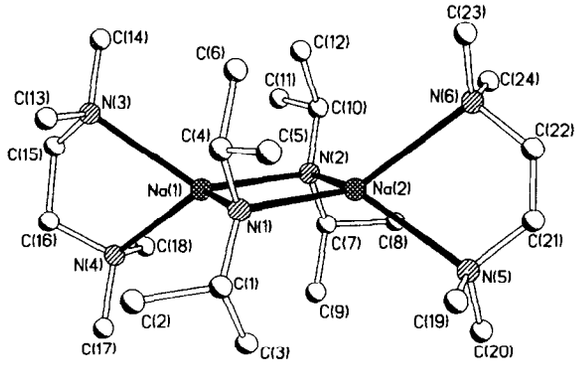

Fig. 1. Molecular structure of the TMEDA adduct of the homoleptic amide **1** without hydrogen atoms and with important atoms labelled.

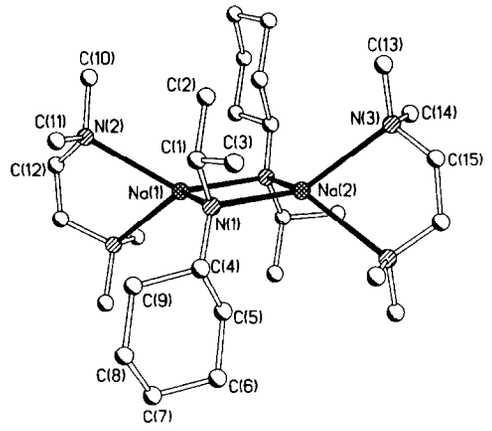

Fig. 2. Molecular structure of the TMEDA adduct of the heteroleptic amide **2** without hydrogen atoms and with important atoms labelled.

conformation. This structural arrangement clearly reduces any steric interactions between R groups and thus aids in the overall stabilisation of the complex. Being derived from a homoleptic amine, **1** differs in the fact that its R groups are all equivalent (^{i}Pr). However, the central feature remains the planar four-membered ring, and it is noticeable from the crystal structure that as a means to reduce steric interactions the methyl groups on the ^{i}Pr units stagger themselves in relation to one another. Although these details may seem pedantic, the one significant departure from this conformational arrangement, the unusual structure of $[PhCH_2(Me)NNa(TMEDA)]_2$ [12], reminds us that everything is not always so simple. Here the organic substituents adopt a *cis* arrangement with an associated buckling of the central ring into a butterfly shape (Fig. 3). From MO geometrical optimisation calculations at the 6.31 G level on the limited model dimer $[Me(H)NNa]_2$ we have found the *cisoid* form, which shows the accompanying ring buckling, to be a less stable structure than that represented by **1** and **2** by a mere 0.03 kcal mol^{-1}

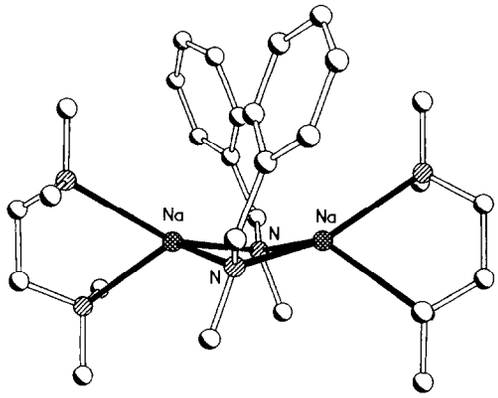

Fig. 3. Alternative molecular structure for a dimeric sodium amide TMEDA adduct exhibiting a *cisoid* arrangement of amido-substituents.

Table 1
Bond lengths (Å) and angles (°) for **1**

Na(1)–N(2)	2.441(2)	Na(1)–N(1)	2.453(2)
Na(1)–N(3)	2.612(2)	Na(1)–N(4)	2.626(2)
Na(2)–N(2)	2.448(2)	Na(2)–N(1)	2.448(2)
Na(2)–N(5)	2.594(2)	Na(2)–N(6)	2.646(2)
N(1)–C(4)	1.446(3)	N(1)–C(1)	1.451(3)
C(1)–C(3)	1.515(4)	C(1)–C(2)	1.522(4)
C(4)–C(6)	1.509(4)	C(4)–C(5)	1.535(4)
N(2)–C(7)	1.447(3)	N(2)–C(10)	1.456(3)
C(7)–C(9)	1.511(3)	C(7)–C(8)	1.527(3)
C(10)–C(12)	1.511(4)	C(10)–C(11)	1.520(4)
N(3)–C(13)	1.451(4)	N(3)–C(14)	1.459(4)
N(3)–C(15)	1.462(4)	N(4)–C(17)	1.462(5)
N(4)–C(16)	1.462(4)	N(4)–C(18)	1.467(4)
C(15)–C(16)	1.503(6)	N(5)–C(19)	1.439(5)
N(5)–C(20)	1.452(4)	N(5)–C(21)	1.453(5)
N(6)–C(23)	1.447(5)	N(6)–C(24)	1.449(4)
N(6)–C(22)	1.458(5)	C(21)–C(22)	1.274(6)
N(2)–Na(1)–N(1)	103.44(7)	N(2)–Na(1)–N(3)	125.98(7)
N(1)–Na(1)–N(3)	114.69(7)	N(2)–Na(1)–N(4)	112.32(7)
N(1)–Na(1)–N(4)	129.07(8)	N(3)–Na(1)–N(4)	71.08(7)
N(2)–Na(2)–N(1)	103.38(7)	N(2)–Na(2)–N(5)	130.43(8)
N(1)–Na(2)–N(5)	111.55(8)	N(2)–Na(2)–N(6)	107.69(7)
N(1)–Na(2)–N(6)	133.45(8)	N(5)–Na(2)–N(6)	71.78(8)
C(4)–N(1)–C(1)	111.4(2)	C(4)–N(1)–Na(2)	114.18(14)
C(1)–N(1)–Na(2)	119.7(2)	C(4)–N(1)–Na(1)	117.7(2)
C(1)–N(1)–Na(1)	113.6(2)	Na(2)–N(1)–Na(1)	76.47(5)
N(1)–C(1)–C(3)	110.6(2)	N(1)–C(1)–C(2)	114.4(3)
C(3)–C(1)–C(2)	107.9(3)	N(1)–C(4)–C(6)	110.3(2)
N(1)–C(4)–C(5)	115.4(3)	C(6)–C(4)–C(5)	108.1(3)
C(7)–N(2)–C(10)	112.1(2)	C(7)–N(2)–Na(1)	116.85(13)
C(10)–N(2)–Na(1)	115.46(14)	C(7)–N(2)–Na(2)	114.97(14)
C(10)–N(2)–Na(2)	116.65(13)	Na(1)–N(2)–Na(2)	76.70(6)
N(2)–C(7)–C(9)	110.6(2)	N(2)–C(7)–C(8)	115.1(2)
C(9)–C(7)–C(8)	107.9(2)	N(2)–C(10)–C(12)	109.9(2)
N(2)–C(10)–C(11)	115.0(2)	C(12)–C(10)–C(11)	108.3(2)
C(13)–N(3)–C(14)	108.8(2)	C(13)–N(3)–C(15)	111.4(3)
C(14)–N(3)–C(15)	109.2(3)	C(13)–N(3)–Na(1)	102.5(2)
C(14)–N(3)–Na(1)	117.9(2)	C(15)–N(3)–Na(1)	106.9(2)
C(17)–N(4)–C(16)	109.1(3)	C(17)–N(4)–C(18)	108.6(3)
C(16)–N(4)–C(18)	111.1(3)	C(17)–N(4)–Na(1)	118.2(2)
C(16)–N(4)–Na(1)	107.3(2)	C(18)–N(4)–Na(1)	102.4(2)
N(3)–C(15)–C(16)	114.7(3)	N(4)–C(16)–C(15)	114.3(3)
C(19)–N(5)–C(20)	109.8(3)	C(19)–N(5)–C(21)	112.6(4)
C(20)–N(5)–C(21)	106.9(4)	C(19)–N(5)–Na(2)	107.8(2)
C(20)–N(5)–Na(2)	114.7(2)	C(21)–N(5)–Na(2)	105.2(2)
C(23)–N(6)–C(24)	109.3(3)	C(23)–N(6)–C(22)	108.7(4)
C(24)–N(6)–C(22)	110.4(4)	C(23)–N(6)–Na(2)	114.5(2)
C(24)–N(6)–Na(2)	109.5(2)	C(22)–N(6)–Na(2)	104.3(2)
C(22)–C(21)–N(5)	126.9(4)	C(21)–C(22)–N(6)	125.3(4)

[12b]. Therefore, the structural preference could easily be strongly influenced by crystal packing forces.

The bond lengths and bond angles for **1** and **2** are presented in full in Tables 1 and 2 respectively, while the bond lengths within the amido N–Na rings themselves are shown for comparative purposes alongside those of other characterised sodium amides in Table 3. In both **1** and **2** the planar rings are almost symmetrical. The range of amido N–Na bond lengths in **1** is only 0.012 Å, and in **2** only 0.005 Å. Also, the sodium

cations in both complexes are four-coordinate, bonding with the two N donor atoms offered by the bidentate TMEDA ligand as well as the two amido Ns. Although four is the most commonly found numerical coordination environment for Li^+ (generally with a distorted tetrahedral geometry), it normally only occurs with sodium in the absence of sufficient coordinating Lewis base(s) or where there is no opportunity for the metal to form internal secondary bonds, i.e. additional intramolecular interactions with the ligand. It is recognised, however, that these highly ionic centres will seek to associate electrostatically with other dimeric units or with donor molecules unless this is precluded by steric effects. In general, alkali metal amides tend to associate laterally as ladders and many examples can be found for lithium amides [23]. Such ladder motifs are also known to exist in potassium chemistry [24]. Despite the close similarity between lithium and sodium structures, there is only one documented case of a sodium amide ladder, that of the polymeric 2,3,4,5-tetramethyl-1-sodiopyrrole [25], excluding the intermetallic ladder $[(LiNa[N(CH_2Ph)_2]_2(OEt)_2)_2]$ [26] which is a special case containing a mixture of Li^+ and Na^+ cations. Some of the most salient examples of electrostatic association in sodium amide chemistry are the extended aggregated structures of $[(Me_2N)_{10}Na_{10}(TMEDA)_4]$, $[(Me_2N)_{12}Na_{12}(TMEDA)_4]$ and $[(Me_2N)_{10}Na_{12}(TMEDA)_4\text{-}(CH_2C_6H_4Me)_2]$ [22], which unexpectedly contain stacking of $(NNa)_2$ ring units. In alkali metal structural chemistry 'ring stacking' is defined as the face-to-face association of $(MN)_2$ rings, while 'ring laddering' is edge-to-edge association. It is obviously the relatively small size of the Me_2N moieties (the smallest diorgano amido group possible) which allows the dimeric units to aggregate to such a high degree, and it is that coupled with the increase in metal ion size in going from Li^+ to Na^+ which causes the mode of association to switch from laddering (as in the Li^+ case) to stacking. For **1** and **2**, therefore, we can only assume that with the Na^+ held in a relatively low coordinate environment further association is sterically prohibited. Increasing the amount of TMEDA available for chelation in the solution had no effect on the solid state structure formed. Sodium, as a result of the size of its larger ionic radius, does, however, have a greater tendency in comparison with lithium to form complexes in which it is five- or six-coordinate if there is opportunity for it to do so. Coupled with increased coordination at the metal centre is the increasing amido N–Na bond lengths, as quite clearly seen from Table 3.

The four-coordination state in **1** and **2** forces the local geometry at Na^+ to be distorted tetrahedral with angles far from the ideal value of 109.5°. The amido N atoms are also approximately tetrahedral, the largest distortion being in the small Na–N–Na angles. Very similar geometries are found in both structures. Indeed, the two molecules are essentially identical except for the replacement of the two ^{i}Pr groups in **1** by two cyclohexyl groups in **2**, even to the extent of the orientations of the substituent groups.

If we now look at the chelate bonding it can be seen that the array of Na–TMEDA bond distances in **1** and **2**, shown in Tables 1 and 2 respectively, is not unusual (cf. that in $[Me(2\text{-}Pyr)NNa(TMEDA)]_2$, 2.511 and 2.510 Å, and in $[(PhCH_2)_2NNa(TMEDA)]_2$, 2.496 and 2.511 Å). What is unusual, however, and this at first might seem surprising, is the manner in which the TMEDA bonds with the metal centres, particularly in the case of NDA. The literature contains many examples of 'normal' bidentate TMEDA → M^+ bonding, that is with the two N atoms donating to a single metal centre, and it would not be an unreasonable assumption to view this as a universal trend. However, an examination of the solution and solid state structural behaviour of the TMEDA complexes of LDA reveals that the chelation here is not the norm. Firstly, the helical polymer of

Table 2
Bond lengths (Å) and angles (°) for **2**

Na(1)–N(1a)	2.443(2)	Na(1)–N(1)	2.443(2)
Na(1)–N(2a)	2.614(2)	Na(1)–N(2)	2.614(2)
Na(2)–N(1a)	2.438(2)	Na(2)–N(1)	2.438(2)
Na(2)–N(3)	2.604(2)	Na(2)–N(3a)	2.604(2)
N(1)–C(1)	1.451(3)	N(1)–C(4)	1.453(3)
C(1)–C(2)	1.514(3)	C(1)–C(3)	1.519(4)
C(4)–C(5)	1.519(3)	C(4)–C(9)	1.526(3)
C(5)–C(6)	1.527(3)	C(6)–C(7)	1.505(4)
C(7)–C(8)	1.517(4)	C(8)–C(9)	1.532(4)
N(2)–C(10)	1.458(4)	N(2)–C(11)	1.461(4)
N(2)–C(12)	1.465(4)	C(12)–C(12a)	1.347(7)
N(3)–C(13)	1.459(3)	N(3)–C(15)	1.463(4)
N(3)–C(14)	1.470(4)	C(15)–C(15a)	1.499(6)
N(1a)–Na(1)–N(1)	103.09(10)	N(1a)–Na(1)–N(2a)	110.46(7)
N(1)–Na(1)–N(2a)	131.30(7)	N(1a)–Na(1)–N(2)	131.30(7)
N(1)–Na(1)–N(2)	110.46(7)	N(2a)–Na(1)–N(2)	71.48(10)
N(1a)–Na(2)–N(1)	103.38(10)	N(1a)–Na(2)–N(3)	110.65(7)
N(1)–Na(2)–N(3)	130.45(7)	N(1a)–Na(2)–N(3a)	130.45(7)
N(1)–Na(2)–N(3a)	110.65(7)	N(3)–Na(2)–N(3a)	72.27(10)
C(1)–N(1)–C(4)	112.3(2)	C(1)–N(1)–Na(2)	115.28(14)
C(4)–N(1)–Na(2)	115.69(13)	C(1)–N(1)–Na(1)	119.61(13)
C(4)–N(1)–Na(1)	112.96(13)	Na(2)–N(1)–Na(1)	76.76(6)
N(1)–C(1)–C(2)	110.1(2)	N(1)–C(1)–C(3)	116.0(2)
C(2)–C(1)–C(3)	108.1(2)	N(1)–C(4)–C(5)	110.3(2)
N(1)–C(4)–C(9)	116.0(2)	C(5)–C(4)–C(9)	107.6(2)
C(4)–C(5)–C(6)	113.2(2)	C(7)–C(6)–C(5)	111.0(2)
C(6)–C(7)–C(8)	111.0(2)	C(7)–C(8)–C(9)	111.3(3)
C(4)–C(9)–C(8)	112.4(2)	C(10)–N(2)–C(11)	108.8(3)
C(10)–N(2)–C(12)	107.7(3)	C(11)–N(2)–C(12)	112.6(3)
C(10)–N(2)–Na(1)	117.5(2)	C(11)–N(2)–Na(1)	104.5(2)
C(12)–N(2)–Na(1)	105.9(2)	C(12a)–C(12)–N(2)	121.3(4)
C(13)–N(3)–C(15)	108.1(2)	C(13)–N(3)–C(14)	108.6(2)
C(15)–N(3)–C(14)	112.3(3)	C(13)–N(3)–Na(2)	117.2(2)
C(15)–N(3)–Na(2)	105.5(2)	C(14)–N(3)–Na(2)	105.2(2)
N(3)–C(15)–C(15a)	114.6(3)		

Symmetry transformations used to generate equivalent atoms: (a) $-x+1, y, -z+3/2$.

crystalline solvent-free LDA is grown from a solution mixture in which two equivalents of TMEDA are available to each metal centre. That no measurable coordination of the Li^+ by TMEDA occurs is unexpected and unusual. However, an LDA complex with TMEDA, grown under different conditions, has been structurally characterised and is also shown to be a polymer, on this occasion though the TMEDA bridges two metal centres in a stretched monodentate manner to give an infinite chain-like structure of linked dimers [6]. This work has also suggested that in solution, in the presence of a relatively high concentration of TMEDA, a dimeric structure can be formed, but is only facile at temperatures below −90°C. However, this dimeric structure is not one which resembles complex **1**, but in fact is one in which Li^+ is three-coordinate and only bonding with one of the two N donor atoms in each TMEDA molecule. A possible explanation for the differences centres upon the relative size of Na^+ in comparison with Li^+. The larger sodium cation can allow for full incorporation of the TMEDA molecule into the dimeric system, while the smaller size of the lithium cation probably exacerbates steric repulsions between the ^{i}Pr groups and the Me groups on the TMEDA molecule. To alleviate steric stress Li^+ relinquishes a possible four-coordination environment by only bonding with one of the N donor atoms, the other remaining essentially free.

The reluctance with which LDA bonds with TMEDA is also reflected in the solution behaviour of NDA. An examination of the chemical shifts of the protons within TMEDA reveals that in benzene-d_6 at room temperature NDA is desolvated, the ethylene protons of TMEDA appearing at a higher frequency (δ 2.13) than the methyl protons (δ 2.08). When TMEDA remains complexed this situation is reversed, as is the case for **2** ($4\times$ Me at δ 2.06, $2\times CH_2$ at δ 2.01) even in the presence of THF which might be expected to aid desolvation of the amide by TMEDA. Presently, the exact nature of the solution state species of **1** is unknown, but it is most likely that the NDA is partially complexed, although we have as yet no spectroscopic evidence for this, or that cyclic or laddered oligomers are formed. It was also noted from the solution NMR studies that the crystal lattices of the two complexes sometimes trapped an amount of unreacted or excess amine. The amount trapped was variable and inconsistent: for **1** this averaged about 12% (highest 50%) and for **2** the highest found was 20%, though these molecules were not seen in the X-ray diffraction studies. Comparing the chemical shifts of the trapped diisopropylamine (DPA) in the NDA complex with that in the lattice of LDA a significant difference is apparent. Free DPA has the signals for Me at δ 0.96 and *CH* at δ 2.85. The DPA entrained in the LDA lattice is consistent with this (δ 0.94 and 2.85 respectively). However, in the NDA case the methyne signal is shifted slightly to δ 2.76 (Me at δ 0.95). Also, the broad *NH* resonance, which in free DPA comes at δ 0.62, moves significantly to the higher frequency value of δ 1.41. These observations could suggest that the DPA is not truly 'free' in the NDA/TMEDA solution, but that it interacts with the Na^+ cation. One clear example of this is the crystal structure of the lithium imide, [Li(cyclohexanone phenylimine). diisopropylamine]$_2$, in which $(^i Pr)_2NH$

Table 3
Comparison of the coordination environment and amido N–Na bond lengths of **1** and **2** with those reported for other structurally characterised sodium amides

Complex	Coordination No. at Na^+	Amido N–Na bond lengths (Å)	Ref.
$[(^iPr)_2NNa(TMEDA)]_2$ **1**	4	2.441(2), 2.453(2)	This work
		2.448(2), 2.448(2)	This work
$[Cy(^iPr)NNa(TMEDA)]_2$ **2**	4	2.438(2), 2.443(2)	This work
$\{^tBu[(F)(^tBu)_2Si]NNa(THF)\}_2$	4	2.483(2), 2.497(2)	[13]
$[((Me)_3Si)_2NNa]_\infty$	2	2.352(2), 2.358(2)	[14]
$[((Me)_3Si)_2N]_3NaEu$	2	2.463(5), 2.484(4)	[15]
$[((Me)_3Si)_2N]_3NaYb$	2	2.450(2), 2.470(2)	[15]
$[(Me_3SiNNa)_2SiMe_2]_3$	2, 3 and 4	2.304(3)–2.601(3)	[16]
$[C_8H_7NNa(TMEDA)]_2$ [a]	4	2.356(5), 2.478(5)	[17]
$[C_8H_7NNa(PMDETA)]_2$ [a]	5	2.474(4), 2.481(5)	[17]
$[Ph(2\text{-}pyr)NNa(PMDETA)]_2$	6	2.499(2), 2.552(2)	[18]
$[Ph(2\text{-}pyr)NNa\frac{3}{2}(HMPA)]_2$	5	2.439(3)	[18]
$[Me(2\text{-}pyr)NNa(TMEDA)]_2$	6	2.446(4), 2.454(5)	[19]
$[PhCH_2(Me)NNa(TMEDA)]_2$	4	2.351(3), 2.392(2)	[12]
$[(PhCH)_2NNa(PMDETA)]$	4	2.384(2)	[20]
$[(PhCH_2)_2NNa(TMEDA)]_2$	4	2.397(2), 2.412(2)	[21]
$[(Me_2N)_{10}Na_{10}(TMEDA)_4]$	4	2.35–2.58	[22]
$[(Me_2N)_{12}Na_{12}(TMEDA)_4]$	4	2.38–2.60	[22]
$[(Me_2N)_{10}Na_{12}(TMEDA)_4(CH_2C_6H_4Me)_2]$	4	2.41–2.60	[22]

[a] Indole derivatives.

acts as Lewis base, donating into the metal centre [27]. Also, mixed complexes where the alkali metal is ligated by both the anion and its protonated counterpart have been structurally characterised, e.g. a lithium piperidide/piperidine composition [28] and a sodium ketimide/ketimine composition [29]. Therefore, it is not unreasonable to assume that a mixed NDA/DPA complex is forming in solution here.

3. Reactivity of NDA

As noted in the Introduction, LDA is an important reagent for organic synthesis, notably as a strong but only weakly nucleophilic base. It is commonly prepared by the reaction of ^{n}BuLi with diisopropylamine, often in a medium containing THF, and used in situ. However, it cleaves THF fairly rapidly, though methods have been devised for preparing and storing it in hydrocarbon–THF mixtures, in which it is more stable. NDA might differ from LDA in its reactivity, and even if its reactivity were similar, it could be an attractive alternative reagent. We have therefore carried out some experiments designed to compare LDA and NDA. Like LDA, NDA cleaves THF fairly rapidly. Its decomposition in THF-d_8 was monitored by NMR, giving a rough estimate of the half-life of ca. 0.9 M NDA in THF-d_8 at the probe temperature as ca. 11 h, and in a THF-d_8–hexane mixture as ca. 3.5 days. Alternatively, solid, unsolvated NDA is readily prepared [11], and appeared to be thermally stable. Our experiments were therefore also designed to test whether the reagent could be stored for long periods.

3.1. Metallation of diphenylmethane

The metallation of diphenylmethane was easily monitored by reaction of the deprotonated species with carbon dioxide to give diphenylacetate, which on acidification gives crystalline diphenylacetic acid:

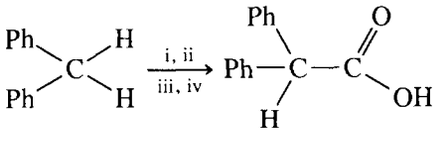

(4)

i = LDA, NDA, NDA(TMEDA) or ^{n}BuLi
ii = THF, cyclohexane/THF
iii = CO_2
iv = acid, H^+

The results of these studies are summarised in Table 4. Note that in this case the comparison could be extended to include butyllithium.

Clearly, the performance of NDA is better than that of LDA over this two-step process, and comparable with that achieved by butyllithium. Moreover, the solid NDA shows only a slow loss of reactivity on storage for over a month. NDA(TMEDA) is even more reactive than NDA, and also loses reactivity only slowly on storage. Similar experiments with other sodium amides (sodium dicyclohexylamide and sodium 2,2,6,6-tetramethylpiperidide) indicated that they too were significantly more reactive than LDA, though slightly less reactive than NDA or NDA(TMEDA) [30].

Table 4
Results from the reaction of diphenylmethane with various metallating reagents yielding diphenylacetic acid on their subsequent reaction with CO_2. All reactions were carried out at ambient temperature (approximately 21°C)

Metallating reagent	Age	Solvent medium	Yield (%)
LDA	fresh	mainly THF	54
^{n}BuLi	fresh	mainly THF	75
NDA	2 days	Cyclohexane/THF	70
NDA	9 days	Cyclohexane/THF	78
NDA	23 days	THF	77
NDA	30 days	Cyclohexane/THF	87
NDA	45 days	Cyclohexane/THF	70
NDA	164 days	Cyclohexane/THF	63
NDA(TMEDA)	3 days	Cyclohexane/THF	87
NDA(TMEDA)	120 days	Cyclohexane/THF	72

3.2. Selective enolate formation

Probably the most important use of LDA is in the formation of enolates from carbonyl compounds. It can be used at low temperatures, which helps to minimise complicating side reactions, and also favours the formation of the kinetic product where alternative sites for deprotonation are available. To compare NDA with LDA we have used methods in which the enolate is trapped by chlorotrimethylsilane (TMSCl) as the silyl enol ether (SEE). For our experiments using 2-octanone, represented by Eq. (5), we used the two-step method of House et al. [31] rather than the 'internal quench' method of Corey and Gross [9], in which the ketone reacts with the base in the presence of TMSCl:

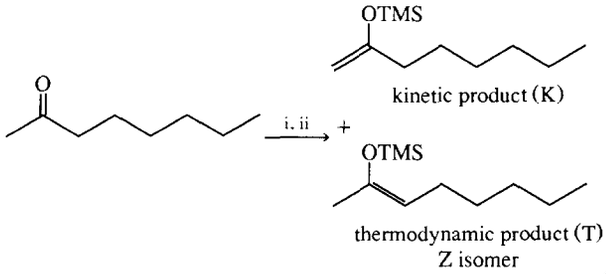

(5)

i = LDA, NDA or NDA(TMEDA), THF
ii = TMSCl

Table 5
Results from the reaction of 2-octanone with various metallating reagents and subsequent trimethylsilylation with TMSCl (all reaction temperatures −78°C) yielding the kinetic (K) and thermodynamic (T) silyl enol ether (SEE) products (SM = starting material)

Metallating reagent	Age	K:T ratio	SEE:SM
LDA	fresh	73.5:26.5	96.3:3.7
NDA	17 days	95.1:4.9	97.4:2.6
NDA	17 days	96:4	95.5:4.5
NDA	60 days	94.6:5.4	97.5:2.5
NDA	60 days	95.6:4.4	97.8:2.2
NDA	135 days	92.6:7.4	92.8:7.2
NDA(TMEDA)	3 days	91.0:9.0	96.3:3.7

For our experiments using 2-methylcyclohexanone, represented by Eq. (6), we used the procedure as described by Brandsma [10]:

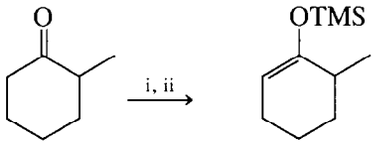

kinetic product (K)

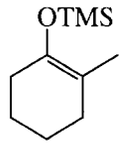

+ (6)

thermodynamic product (T)

i = LDA, NDA or NDA(TMEDA), THF
ii = TMSCl

The results for the reactions of 2-octanone and 2-methylcyclohexanone are set out in Tables 5 and 6.

The most noteworthy feature of the reactions with 2-octanone (Table 5) is the high conversion and selectivity achieved with NDA and NDA(TMEDA), even with the two-step procedure. With this procedure, House et al. [31] obtained high selectivity with LDA, but only at ca. 50% conversion; as shown in entry 1 of Table 5, high conversion is obtainable, but only at the expense of

Table 6
Results from the reaction of 2-methylcyclohexanone with various metallating reagents (all reaction temperatures −78°C) and subsequent trimethylsilylation with TMSCl (−50°C) yielding the kinetic (K) and thermodynamic (T) silyl enol ether (SEE) products (SM = starting material)

Metallating reagent	Age	K:T ratio	SEE:SM
LDA	*in situ*	94.9:5.1	96.5:3.5
NDA	10 days	93.6:6.4	95.1:4.9
NDA	28 days	95.1:4.9	91.0:9.0
NDA	30 days	95.7:4.3	92.7:7.3
NDA	56 days	94.9:5.1	92.2:7.8
NDA	150 days	96.6:3.4	92.9:7.1
NDA(TMEDA)	3 days	94.1:5.9	94.5:5.5

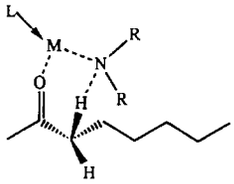

4

Fig. 4. A possible transition state in the metal amide deprotonation of 2-octanone.

selectivity. It should be noted, however, that we have confirmed Corey and Gross's [9] observation that by the internal quench procedure both high conversion and selectivity are obtainable. The retention of the reactivity of NDA on storage was also again demonstrated. The reactions with 2-methylcyclohexanone (Table 6) again demonstrate that NDA has reactivity and selectivity at least as good as that of LDA.

One possible conclusion that can be drawn from these results is that the degree of steric interference between the ^{i}Pr groups and the larger organic groups of the ketone is not reduced by the use of a larger metal and hence longer M–N bond. Given a transition state of the type depicted in Fig. 4 for 2-octanone, we would predict that a loss in selectivity would only occur from a decrease in steric bulk in the organic portion of the metallating species. Thus, $[(Me)_2NNa(L)]_n$ would most likely have lower selectivity but so also would $[(Me)_2NLi(L)]_n$, though probably to a lesser degree given the different sizes of the metal cations and M–N bonds.

4. Conclusions

In reactions where a high degree of reactivity is required of the deprotonating/metallating reagent, then the use of heavier alkali metal organyls or amides can be advantageous. Where the mechanism is kinetically or thermodynamically controlled, a loss of selectivity will not always necessarily accompany the use of sodium rather than lithium complexes. However, it would be a mistake to assume that the nature of the metal is not important when utilising these reagents; clearly in the selective enolate formation at the heart of the discrepancy between the results for NDA and LDA in the two-step reactions must lie the metallic cation. Therefore, it would be prudent to isolate and characterise not only the metallating reagent itself, for all the reasons given in the Introduction, but also the metallated precursor. That most sodium amides are easily synthesised, relatively easy to manipulate and soluble in hydrocarbon solvents in the presence of sufficient coordinating donor molecules (normally a stoichiometric amount) should allow for further development not only in their

isolation and characterisation but also now in their role as important organometallic reagents. A role comparable perhaps with that now occupied by the commercial lithium reagents ^{n}BuLi and LDA.

5. Experimental

Prior to their usage all solvents and reagents were dried. The amines and Lewis bases were distilled and stored over 4A molecular sieves. Hexane, cyclohexane and THF were dried by reflux over Na wire and degassed immediately before use. Standard inert atmosphere and Schlenk techniques were utilised throughout. ^{n}BuNa was prepared from the reaction of ^{n}BuLi and Na^{t}BuO (1 : 1) in hexane, dried in vacuo and stored and handled in an argon atmosphere glove box. All NMR spectra were recorded on a Bruker AMX400 and the chemical shifts internally referenced and quoted relative to δ 0.00 for $SiMe_4$.

5.1. Synthesis and characterisation of 1, [(^{i}Pr)$_2$NNa-(TMEDA)]$_2$

(i) Diisopropylamine (1.31 ml, 10 mmol) was added dropwise to a stirred, chilled suspension of ^{n}BuNa (0.80 g, 10 mmol) in 10 ml of hexane. After 10 min stirring the reaction was complete and a white precipitate formed. Addition of TMEDA (3.02 ml, 20 mmol) followed by gentle heating ensured complete dissolution. The pale orange solution was filtered and allowed to stand at ambient temperature for 24 h before yielding a crop of pale red crystals. The crystals were isolated by filtration, washed with hexane and dried in vacuo. Yield 31%.

(ii) To sodium metal dispersed in toluene or octane (74 mmol, 30% w/w) was added, under argon, diisopropylamine (105 mmol, 13.8 ml), isoprene (105 mmol, 10.5 ml) and TMEDA (75 mmol, 11.3 ml) in hexane (35 ml). The exothermic reaction gradually produced a red solution as the sodium metal disappeared. After filtration, red crystals were grown at 4°C. Yield 75%. Melting point 89–94°C.

Anal. Found: C, 60.3; H, 13.1; N, 17.3; Na, 9.1. Calc.: C, 60.3; H, 12.6; N, 17.6; Na, 9.6%.

IR spectrum (Nujol mull, cm^{-1}) (s = strong, m = medium, w = weak, br = broad): 2920 s(br), 2720 s, 2620 w, 2600 s, 2545 s, 1550 m, 1460 s, 1360 s, 1342 s, 1315 s, 1295 s, 1255 s, 1180 w, 1160 s, 1150 w, 1100 m, 1081 s, 1041 s, 1020 s, 1000 s, 950 s, 920 m, 910 w, 890 s, 820 m, 785 s, 720 w.

NMR data (400 MHz, 298 K, benzene-d_6): ^{1}H δ 3.66 (2H, septet, CH), δ 2.13 (4H, s, TMEDA(CH_2)), δ 2.08 (12H, s, TMEDA(CH_3)), δ 1.26 (12H, d, Me). ^{13}C (100.6 MHz): δ 58.33 (TMEDA(CH_2)), δ 51.07 (CH), δ 46.50 (TMEDA(Me)), δ 28.84 (Me).

5.2. Synthesis and characterisation of 2, [Cy(^{i}Pr)NNa-(TMEDA)]$_2$

Isopropylcyclohexylamine (1.67 ml, 10 mmol) was added to a cooled, stirred suspension of ^{n}BuNa (0.80 g, 10 mmol) in hexane (5 ml). The reaction mixture was stirred for 15 min giving a peach coloured suspension. Addition of TMEDA (1.51 ml, 10 mmol) followed by vigorous heating resulted in a dark brown solution. On cooling slowly from 55°C this afforded a large crop of pale pink crystals. The crystals were isolated by filtration, washed with hexane and dried in vacuo. Yield 76%. Melting point 96–97°C.

IR spectrum (Nujol mull, cm^{-1}) (s = strong, m = medium, w = weak, br = broad, sh = shoulder): 2910 s, br, 2840 s, 2780 s, br, 2700 s, 2530 m, sh, 2520 m, 1540 w, br, 1470 m, sh, 1465 s, sh, 1450 s, 1410 m, 1375 m, 1355 m, 1330 m, 1320 m, 1310 m, 1290 s, 1285 m, sh, 1255 w, sh, 1250 w, 1230 w, 1175 m, 1150 s, 1130 m, 1105 m, 1080 m, sh, 1075 m, 1060 w, 1030 m, 1020 s, 995 w, 955 w, sh, 945 m, 930 m, 910 m, 890 w, 880 w, 840 w, 805 w, 780 m, 770 w, sh, 720 w.

NMR data (400 MHz, 298 K, THF-d_8): ^{1}H δ 3.68 (1H, septet, CH), δ 2.98 (1H, tt, CH), δ 2.24 (2H, m, CH), δ 2.06 (12H, s, TMEDA(Me)), δ 2.01 (4H, s, TMEDA(CH_2)), δ 1.93 (2H, m, CH), δ 1.85 (1H, m, CH), δ 1.59 (2H, m, CH), δ 1.34 (1H, m, CH), δ 1.21, 1.20 (6H, d, Me), δ 0.84 (2H, m, CH). ^{13}C (100.6 MHz, 298 K, toluene-d_8): δ 62.15 (Me), 58.24 (CH), δ 50.94 (CH), δ 46.55 (NMe), δ 40.89 (CH_2), δ 35.12 (CH_2), 29.14 (Me), δ 28.65 (CH_2), δ 27.80 (CH_2), δ 27.43 (CH_2), δ 24.32 (CH). Assignments verified by *J*-mod experiments [32].

5.3. Crystal structure analyses

Crystal data for **1**: $C_{24}H_{60}N_6Na_2$, $M = 478.8$, monoclinic, space group $P2_1$, $a = 8.6329(10)$, $b = 19.119(3)$, $c = 10.3903(14)$ Å, $\beta = 108.025(9)°$, $V = 1630.8(4)$ Å^3, $Z = 2$, $D_c = 0.975$ g cm^{-3}, $\mu = 0.676$ mm^{-1} for Cu Kα radiation ($\lambda = 1.54184$ Å), $F(000) = 536$, $T = 240$ K. Unit cell parameters were refined from 2θ values (30–40°) of 32 reflections measured at $\pm\omega$ on a Stoe–Siemens diffractometer. Intensities were measured with ω–θ scans and an on-line profile fitting procedure [33], from a crystal of size 0.65 × 0.42 × 0.29 mm^3. No significant variation was observed in the intensities of three standard reflections monitored at regular intervals. The structure was determined by direct methods [34] and refined on F^2 by full-matrix least-squares methods [35] from 5306 independent reflections ($2\theta = 130°$, 7811 reflections measured, $R_{int} = 0.0287$), with a weighting scheme $w^{-1} = \sigma^2(F_o^2) + (aP)^2 + (bP)$, where $P = (F_o^2 + 2F_c^2)/3$, $a = 0.0697$, $b = 0.2772$. Hydrogen atoms were included at calculated positions and made to ride on their parent carbon

atom with isotropic displacement parameters tied to the equivalent values for these atoms. All other atoms were assigned anisotropic displacement parameters. No absorption corrections were applied; an isotropic extinction parameter x was refined to 0.0075(6), such that F_c is multiplied by $(1 + 0.001xF_c^2\lambda^3/\sin 2\theta)^{-1/4}$. All shift/e.s.d. ratios were less than 0.002 in the final refinement cycle. The enantiopole parameter [36] refined to 0.05(6), indicating the correct polar axis direction. For all reflections, $R_w = [\sum w(F_o^2 - F_c^2)^2/\sum w(F_o^2)^2]^{1/2} = 0.1246$; the conventional $R = 0.0432$ for F values of 4936 reflections with $F_o^2 > 2\sigma(F_o^2)$; goodness of fit 1.044 on F^2 values for all data and 306 refined parameters. All features in a final difference synthesis lie between +0.23 and −0.22 e Å^{-3}.

Crystal data for **2**: $C_{30}H_{68}N_6Na_2$, $M = 558.9$, monoclinic, space group $C2/c$, $a = 15.878(5)$, $b = 13.658(4)$, $c = 17.574(6)$ Å, $\beta = 106.25(2)°$, $V = 3659(2)$ Å^3, $Z = 4$, $D_c = 1.015$ g cm^{-3}, $\mu = 0.662$ mm^{-1} for Cu Kα radiation ($\lambda = 1.54184$ Å), $F(000) = 1248$, $T = 240$ K. Measurements were made as for **1** ($2\theta = 25–40°$) for cell refinement, crystal size 0.71 × 0.63 × 0.27 mm^3. The structure was determined and refined as above from 3041 independent reflections ($2\theta_{max} = 130°$, 4024 reflections measured, $R_{int} = 0.0858$), with weighting parameters $a = 0.0907$, $b = 2.0114$. The molecule lies on a two-fold rotation axis passing through both sodium atoms. Extinction parameter $x = 0.00045(14)$. $R_w = 0.1715$ for all reflections, conventional $R = 0.0529$ for F values of 2073 reflections with $F_o^2 > 2\sigma(F_o^2)$; goodness of fit 1.040 for 180 parameters. All features in a final difference synthesis lie between +0.35 and −0.25 e Å^{-3}.

For both structures, tables of anisotropic displacement parameters and hydrogen atom coordinates have been deposited at the Cambridge Crystallographic Data Centre. Non-hydrogen atom coordinates and equivalent isotropic displacement parameters for **1** and **2** are given in Tables 7 and 8 respectively.

Table 7
Atomic coordinates (×10^4) and equivalent isotropic displacement parameters (Å^2 × 10^3) for **1**

Atom	x	y	z	U_{eq}
Na(1)	2948.6(10)	976.8(4)	8066.0(8)	49.1(2)
Na(2)	2358.6(10)	2090.5(4)	5888.4(8)	47.5(2)
N(1)	2514(2)	2234.6(9)	8266(2)	48.6(4)
C(1)	3900(3)	2592(2)	9188(3)	62.6(6)
C(2)	4163(5)	2439(3)	10677(3)	112(2)
C(3)	5452(3)	2405(2)	8877(3)	78.4(8)
C(4)	1003(3)	2452.9(14)	8470(3)	58.7(6)
C(5)	589(5)	3232(2)	8220(5)	106.5(13)
C(6)	−402(3)	2034(2)	7576(3)	74.4(7)
N(2)	2846(2)	838.8(9)	5705(2)	45.5(4)
C(7)	4359(3)	667.3(13)	5454(2)	52.3(5)
C(8)	4352(4)	769(2)	3995(3)	80.4(9)
C(9)	5745(3)	1094(2)	6359(3)	66.5(7)
C(10)	1487(3)	427.2(12)	4869(2)	54.5(5)
C(11)	1686(4)	−360(2)	5048(4)	88.5(10)
C(12)	−65(3)	638(2)	5149(3)	71.7(7)
N(3)	1495(3)	178.6(12)	9379(2)	61.9(5)
N(4)	5121(3)	153.8(14)	9696(2)	69.7(6)
C(13)	1286(4)	647(2)	10411(3)	81.1(8)
C(14)	−86(4)	−116(2)	8630(3)	83.2(9)
C(15)	2622(5)	−390(2)	9973(4)	94.2(11)
C(16)	4356(5)	−166(2)	10626(3)	93.2(11)
C(17)	6684(4)	457(2)	10476(4)	103.4(12)
C(18)	5412(5)	−368(2)	8761(3)	84.8(9)
N(5)	3559(3)	3163.8(13)	4999(2)	70.2(6)
N(6)	230(3)	2495.9(12)	3580(2)	70.1(6)
C(19)	3652(7)	3733(2)	5927(5)	121(2)
C(20)	5146(5)	3047(2)	4828(5)	106.9(13)
C(21)	2430(6)	3303(3)	3662(6)	157(3)
C(22)	931(7)	3134(3)	3226(5)	153(2)
C(23)	−1374(5)	2653(3)	3666(5)	124(2)
C(24)	96(5)	1964(2)	2558(3)	98.2(11)

U_{eq} is defined as one third of the trace of the orthogonalized U_{ij} tensor.

Table 8
Atomic coordinates (×10^4) and equivalent isotropic displacement parameters (Å^2 × 10^3) for **2**

Atom	x	y	z	U_{eq}
Na(1)	5000	5758.6(8)	7500	44.9(3)
Na(2)	5000	3539.7(8)	7500	43.1(3)
N(1)	6197.0(11)	4646.3(13)	7475.6(10)	43.2(4)
C(1)	6500(2)	4588(2)	6770.3(14)	53.0(6)
C(2)	5724(2)	4597(2)	6035.7(14)	62.9(7)
C(3)	7069(3)	3711(3)	6719(2)	105.6(14)
C(4)	6918.2(14)	4683(2)	8197.9(13)	47.0(5)
C(5)	6574(2)	4609(2)	8920.1(13)	51.7(6)
C(6)	7302(2)	4570(2)	9699.9(14)	63.8(7)
C(7)	7892(2)	5451(2)	9789(2)	75.4(8)
C(8)	8248(2)	5562(3)	9078(2)	87.0(11)
C(9)	7505(2)	5587(2)	8303(2)	70.9(8)
N(2)	5041(2)	7312(2)	6642.5(13)	66.5(6)
C(10)	4417(3)	7359(3)	5857(2)	94.4(11)
C(11)	5931(3)	7325(3)	6557(2)	99.0(12)
C(12)	4866(4)	8145(2)	7101(2)	145(2)
N(3)	4406(2)	2000(2)	6644.3(12)	57.8(6)
C(13)	4457(2)	2000(2)	5828(2)	71.4(8)
C(14)	3479(2)	1926(2)	6634(2)	77.2(9)
C(15)	4929(3)	1179(2)	7060(2)	85.5(10)

U_{eq} is defined as one third of the trace of the orthogonalized U_{ij} tensor.

5.4. Metallation of diphenylmethane

At room temperature diphenylmethane (3 mmol) was added to a solution of the metallating agent (3.3 mmol) in cyclohexane (5 ml) and THF (2 ml) (or other solvent systems as listed in Table 4). The resulting solution was then stirred for 30 min before it was poured onto solid CO_2, which was then allowed to slowly evaporate. A solution of 1 M NaOH was then added, followed by Et_2O, and the aqueous layer separated and acidified to

pH 1. The resulting product was extracted into Et_2O, dried and concentrated in vacuo. The product was diphenylacetic acid which was dried and weighed until constant weight and melting point. (Literature melting point, 148°C).

5.5. Enolate formation from 2-octanone

To a solution of the metallating agent (3 mmol) in THF (15 ml) at −78°C was added 2-octanone (2.7 mmol) and the resulting solution was stirred at this temperature for 10 min. TMSCl (3 mmol) was added and the solution allowed to warm to room temperature and stirred for a further 90 min before being quenched with aqueous $NaHCO_3$. It was then extracted with hexane and the extract dried over $MgSO_4$ and concentrated in vacuo. The residue was analysed by GC/MS.

5.6. Enolate formation from 2-methylcyclohexanone

2-Methylcyclohexanone (0.98 mmol) was added at −78°C to a THF (10 ml) solution of the metallating agent (1.1 mmol). The mixture was then allowed to warm slowly to −50°C at which point TMSCl (1.3 mmol) was added and the resulting solution again allowed to warm up slowly until it was at room temperature. Diethylamine (0.4 mmol) was added and after 15 min stirring the reaction mixture was poured into ice water and the product extracted into hexane (3 × 15 ml). The combined organic extracts were washed with saturated ammonium chloride solution and dried with $MgSO_4$. The silyl enol ether products were concentrated in vacuo and subsequently analysed by GC/MS.

5.7. GC / MS details

A Finnigan ion trap detector interfaced to a Carlo-Erba 5300 gas chromatograph was employed to analyse all organic products. The following GC/MS conditions were used. Column: 30 m PTE5 0.32 i.d. capillary column. Carrier gas: helium. Oven: 40°C 1 min + 20°C min^{-1} to 250°C hold. Injection: 0.1 μl cold on column with CH_2Cl_2 as solvent. Retention times: Reaction 5.5, 2-octanone 287 s, kinetic product 370 s, thermodynamic product (Z isomer) 374 s, thermodynamic product (E isomer) 383 s; Reaction 5.6, 2-methylcyclohexanone 254 s, kinetic product 340 s, thermodynamic product 357 s.

Acknowledgements

We thank the SERC (EPSRC) and Associated Octel Ltd. (Ellesmere Port) for sponsoring this collaborative research project.

References and notes

[1] K. Gregory, P.v.R. Schleyer and R. Snaith, *Adv. Inorg. Chem.*, *37* (1991) 47. R.E. Mulvey, *Chem. Soc. Rev.*, *20* (1991) 167.
[2] C.H. Heathcock, in J.D. Morrison (ed.), *Asymmetric Synthesis*, Vol. 3B, Academic Press, New York, 1984. G.B. Gill and D.A. Whiting, *Aldrichim. Acta*, *19* (1986) 31. J.L. Wardell, in F.R. Hartley (ed.), *The Chemistry of the Metal–Carbon Bond*, Vol. 4, Wiley, Chichester, UK, 1987. B.J. Wakefield, *Organolithium Methods*, Academic Press, San Diego, 1988.
[3] A.S. Galiano-Roth and D.B. Collum, *J. Am. Chem. Soc.*, *111* (1989) 6722. A.S. Galiano-Roth, Y.-J. Kim, J.H. Gilchrist, A.T. Harrison, D.J. Fuller and D.B. Collum, *J. Am. Chem. Soc.*, *113* (1991) 5053. P.L. Hall, J.H. Gilchrist, A.T. Harrison, D.J. Fuller and D.B. Collum, *J. Am. Chem. Soc.*, *113* (1991) 9575. J.H. Gilchrist and D.B. Collum, *J. Am. Chem. Soc.*, *114* (1992) 794.
[4] P.G. Williard and M.J. Hintze, *J. Am. Chem. Soc.*, *109* (1987) 5539. W. Zarges, M. Marsch, K. Harms and G. Boche, *Angew. Chem., Int. Ed. Engl.*, *28* (1989) 1392.
[5] N.D.R. Barnett, R.E. Mulvey, W. Clegg and P.A. O'Neil, *J. Am. Chem. Soc.*, *113* (1991) 8187.
[6] M.P. Bernstein, F.E. Romesberg, D.J. Fuller, A.T. Harrison, D.B. Collum, Q.-Y. Lui and P.G. Williard, *J. Am. Chem. Soc.*, *114* (1992) 5100.
[7] P.G. Williard and J.M. Salvano, *J. Org. Chem.*, *58* (1993) 1.
[8] F.S. Mair, W. Clegg and P.A. O'Neil, *J. Am. Chem. Soc.*, *115* (1993) 3388 (see also Ref. [4]).
[9] E.J. Corey and A.W. Gross, *Tetrahedron. Lett.*, *25* (1984) 495.
[10] L. Brandsma, *Preparative Polar Organometallic Chemistry*, Vol. 2, Springer, 1990.
[11] D. Barr, A.J. Dawson and B.J. Wakefield, *J. Chem. Soc., Chem. Commun.*, (1992) 204.
[12] (a) P.C. Andrews, D.R. Armstrong, W. Clegg, M. MacGregor and R.E. Mulvey, *J. Chem. Soc., Chem. Commun.*, (1991) 497. (b) P.C. Andrews, *PhD Thesis*, University of Strathclyde, 1992.
[13] U. Pieper, D. Stalke, S. Vollbrecht and U. Klingebiel, *Chem. Ber.*, *123* (1990) 1039.
[14] R. Grunning and J.L. Atwood, *J. Organomet. Chem.*, *137* (1977) 101.
[15] T.D. Tilley, R.A. Anderson and A. Zalkin, *Inorg. Chem.*, *23* (1984) 2271.
[16] D.J. Brauer, H. Burger, W. Geschwandtner, G.R. Liewald and C. Kruger, *J. Organomet. Chem.*, *248* (1983) 1.
[17] K. Gregory, M. Bremer, P.v.R. Schleyer, N.P. Lorenzen, J. Kopf and E. Weiss, *Organometallics*, *9* (1990) 1485.
[18] P.C. Andrews, W. Clegg and R.E. Mulvey, *Angew. Chem., Int. Ed. Engl.*, *29* (1990) 1440.
[19] P.C. Andrews, D.R. Baker, W. Clegg, R.E. Mulvey and P.A. O'Neil, *Polyhedron*, *10* (1991) 1839.
[20] P.C. Andrews, R.E. Mulvey, W. Clegg and P.A. O'Neil, *J. Organomet. Chem.*, *386* (1990) 287.
[21] P.C. Andrews, D.R. Armstrong, D.R. Baker, R.E. Mulvey, W. Clegg, L. Horsburgh, P.A. O'Neil and D. Reed, *Organometallics*, *14* (1995) 427.
[22] N.P. Lorenzen, J. Kopf, F. Olbrich, U. Schümann and E. Weiss, *Angew. Chem., Int. Ed. Engl.*, *29* (1990) 1441.
[23] D.R. Armstrong, D. Barr, W. Clegg, S.M. Hodgson, R.E. Mulvey, D. Reed, R. Snaith and D.S. Wright, *J. Am. Chem. Soc.*, *111* (1989) 4719.
[24] P.C. Andrews, W. Clegg, R.E. Mulvey, P.A. O'Neil and H.M.M. Wilson, *J. Chem. Soc., Chem. Commun.*, (1993) 1142.
[25] N. Kuhn, G. Henkel and J. Kreutzberg, *Angew. Chem., Int. Ed. Engl.*, *29* (1990) 1143.
[26] D.R. Baker, R.E. Mulvey, W. Clegg and P.A. O'Neil, *J. Am. Chem. Soc.*, *115* (1993) 6472.

[27] R.A. Wanat, D.B. Collum, G. van Duyne, J. Clardy and R.T. Depue, *J. Am. Chem. Soc., 108* (1986) 3415.
[28] G. Boche, I. Langlotz, M. Marsch, K. Harms and N.E.S. Nudelman, *Angew. Chem., Int. Ed. Engl., 31* (1992) 1205.
[29] W. Clegg, M. MacGregor, R.E. Mulvey and P.A. O'Neil, *Angew. Chem., Int. Ed. Engl., 31* (1992) 93.
[30] D. Barr and L. Cowton, unpublished results.
[31] H.O. House, L.J. Czuby, M. Gall and H.D. Olmstead, *J. Org. Chem., 34* (1971) 2324. H.O. House, M. Gall and H.D. Olmstead, *J. Org. Chem., 36* (1971) 2361.
[32] *J*-modulated spin-echo experiments. For an explanation see H. Friebolin, *Basic One- and Two-Dimensional NMR Spectroscopy*, VCH, New York, 1993, p. 187.
[33] W. Clegg, *Acta Crystallogr., Sect. A, 37* (1981) 22.
[34] G.M. Sheldrick, *SHELXTL User's Manual*, Siemens Analytical X-ray Instruments Inc., Madison, WI, 1990.
[35] G.M. Sheldrick, *SHELXL 93, Program for Crystal Structure Refinement*, University of Göttingen, Germany, 1993.
[36] H.D. Flack, *Acta Crystallogr., Sect. A, 39* (1983) 876.